Identification of Genes Required for Apical Protein Trafficking in *Drosophila* Photoreceptor Cells

Azadeh Laffafian and Ulrich Tepass[1]
Department of Cell and Systems Biology, University of Toronto, Ontario M5S 3G5, Canada
ORCID ID: 0000-0002-7494-5942 (U.T.)

ABSTRACT *Drosophila melanogaster* photoreceptor cells are highly polarized epithelial cells. Their apical membrane is further subdivided into the stalk membrane and the light-sensing rhabdomere. The photopigment Rhodopsin1 (Rh1) localizes to the rhabdomere, whereas the apical determinant Crumbs (Crb) is enriched at the stalk membrane. The proteoglycan Eyes shut (Eys) is secreted through the apical membrane into an inter-rhabdomeral space. Rh1, Crb, and Eys are essential for the development of photoreceptor cells, normal vision, and photoreceptor cell survival. Human orthologs of all three proteins have been linked to retinal degenerative diseases. Here, we describe an RNAi-based screen examining the importance of 237 trafficking-related genes in apical trafficking of Eys, Rh1, and Crb. We found 28 genes that have an effect on the localization and/or levels of these apical proteins and analyzed several factors in more detail. We show that the Arf GEF protein Sec71 is required for biosynthetic traffic of both apical and basolateral proteins, that the exocyst complex and the microtubule-based motor proteins dynein and kinesin promote the secretion of Eys and Rh1, and that Syntaxin 7/Avalanche controls the endocytosis of Rh1, Eys, and Crb.

Drosophila photoreceptor cells (PRCs) are an important model for the epithelial differentiation of a sensory cell and to study vesicle trafficking and neuro-degeneration (for reviews see Tepass and Harris 2007; Shieh 2011; Xiong and Bellen 2013; Schopf and Huber 2017). PRCs have specialized apical and basolateral membranes that are segregated by an epithelial adherens junction, the zonula adherens. While the basolateral membrane extends an axon, the apical membrane differentiates a light sensing organelle, the rhabdomere. In addition to the rhabdomere, the apical membrane of PRCs contains the stalk membrane domain that connects the rhabdomere to the zonula adherens. Here, we have identified factors that contribute to the trafficking of three proteins - Rhodopsin 1 (Rh1), Crumbs (Crb), and Eyes shut (Eys) to the apical membrane of PRCs to further our understanding of how the vesicle trafficking machinery

contributes to the maintenance and function of a complex epithelial sensory cell.

Rhodopsin photopigments are seven-pass *trans*-membrane G-protein-coupled receptors localized at rhabdomeres, an array of 10th of thousands tightly packed microvilli. The main rhodopsin protein, Rh1, is found in PRCs R1 to R6. Mutations in rhodopsin and defects in its trafficking are the most frequent cause of retinal degenerative diseases in flies and humans (Colley *et al.*, 1995; Xiong and Bellen 2013; Nemet *et al.*, 2015).

The apical polarity determinant Crumbs (Crb) is found at the stalk membrane. This transmembrane protein is important in regulating the length of the stalk; a reduction of Crb limits and an overexpression of Crb expands the stalk membrane (Pellikka *et al.*, 2002). Crb is also important in the maintenance of the zonula adherens, and the proper distal to proximal elongation of rhabdomeres (Pellikka *et al.*, 2002; Izaddoost *et al.*, 2002). *crb* mutant PRCs show light-induced degeneration (Johnson *et al.*, 2002) and a human homolog of Crb (CRB1) has been linked to the retinal degenerative diseases, retinitis pigmentosa (RP12) and Leber congenital amaurosis (LCA8) (den Hollander *et al.*, 1999, Richard *et al.*, 2006; den Hollander *et al.*, 2008; Bujakowska *et al.*, 2012; Pellikka and Tepass 2017).

The apical membranes of PRCs face a luminal space called the interrhabdomeral space (IRS). The IRS is important in vision in flies as it physically separates, and therefore optically isolates the rhabdomeres within one ommatidium from each other. The proteoglycan Eys shut

(Eys) is essential in the formation of the IRS (Husain *et al.*, 2006; Zelhof *et al.*, 2006). Eys is thought to be secreted through the stalk membrane into the IRS (Husain *et al.*, 2006). Similar to mutations in rhodopsin and CRB1, also mutations in human EYS have been linked to retinal degenerative diseases such as retinitis pigmentosa (RP25) (Abd El-Aziz *et al.*, 2008; Collin *et al.*, 2008).

The fact that several apical transmembrane or secreted proteins play key roles in PRC development and disease motivates a careful assessment of the mechanism that transport and target these proteins. Several factors have been identified that are involved in apical trafficking in *Drosophila* PRCs (see Figure 1). Examples include Rab1 and Syntaxin 5 (Syx5) that are essential in ER to Golgi trafficking (Satoh *et al.*, 1997; Satoh *et al.*, 2016). Rab6 is important in the exit of apical proteins from the Golgi (Iwanami *et al.*, 2016) and Rab11, Rip11, Myosin V and the exocyst complex (*e.g.*, Sec6) are important in the secretion of Rh1 and other rhabdomeral proteins (Satoh *et al.*, 2005; Li *et al.*, 2007; Beronja *et al.*, 2005). Secretory vesicle carrying Rh1 and other rhabdomere-destined proteins are moved along actin fibers of the rhabdomere terminal web driven by the Myosin V motor (Li *et al.*, 2007). Myosin V interacts with Crb to facilitate normal Rh1 transport to the rhabdomere (Pocha *et al.*, 2011). Following the path of Rh1, once at the rhabdomeres, Rab5 and Shibire/Dynamin (Shi) are required for its endocytosis (Satoh *et al.*, 2005; Alloway *et al.*, 2000; Kiselev *et al.*, 2000). Some of this endocytosed Rh1 is recycled back to the rhabdomere through a retromer-dependent pathway that involves the retromer protein Vps26, whereas the rest is sent to the lysosome for degradation (Wang *et al.*, 2014; Chinchore *et al.*, 2009).

It appears that the apical and basolateral trafficking routes diverge somewhere along the Golgi prior to the action of Rab6, whereas the rhabdomeral *vs.* stalk membrane route diverges downstream of Rab6 following the exit from the Golgi. Crb and Eys are thought to be targeted to the stalk through a pathway distinct from the secretory pathway used by rhabdomeral proteins (Beronja *et al.*, 2005, Husain *et al.*, 2006). The components involved in Crb and Eys exocytosis are currently unknown, except for evidence suggesting that microtubules and microtubule motor proteins are involved in Crb localization during pupal stages (Mukhopadhyay *et al.*, 2010; Chen *et al.*, 2010; League and Nam 2011; Mui *et al.*, 2011; Nam 2016).

To develop a better understanding of the apical trafficking mechanisms that control the distribution of Eys, Crb, and Rh1 in the fly retina we analyzed 237 candidate genes, known or predicted to encode proteins involved in vesicle trafficking. We identified 28 genes that are important for the localization or concentration of apical proteins, and provide a more detail analysis of four factors: The Arf guanine nucleotide exchange factor (GEF) Sec71, the exocyst complex, the microtubule motor dynein, and the endocytotic regulator Syntaxin 7 (Syx7)/Avalanche (Avl).

MATERIALS AND METHODS

Drosophila stocks and crosses
UAS-RNAi lines were obtained from the Bloomington *Drosophila* Stock Center (BDSC) and Vienna *Drosophila* Resource Center (VDRC). See Table S1 for a list of lines used. UAS-RNAi constructs were expressed in the developing eye with UAS-Dicer-2 GMR-Gal4. GMR-Gal4 activity starts in the developing retina posterior to the morphogenetic furrow at third larval instar and continues to adulthood (Freeman 1996). UAS-Dicer-2 was used to amplify the effects of RNAi (Ketting *et al.*, 2001). Flies were raised at 25° under dark conditions. 0-24 hr old adult progeny were analyzed. We used UAS-Dicer-2/+; pGMR-Gal4/+ as control for all experiments.
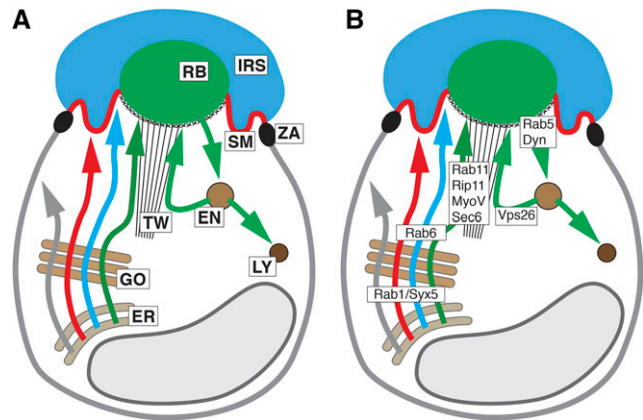
Figure 1 Structure and trafficking of *Drosophila* PRCs. (A) Schematic of PRC showing major known trafficking pathways. Arrows highlight basolateral (gray) and apical (red, Crb; blue, Eys; green, Rh1) trafficking pathways. Abbreviations: EN, endosome; ER, endoplasmatic reticulum; GO, Golgi apparatus; IRS, interrhabdomeral space; LY, lysosome; RB, rhabdomere; SM, stalk membrane; TW, terminal web; ZA, zonula adherens. (B) Schematic of PRC showing site of action of major known vesicle trafficking factors. See text for description.

Transmitted Light Illumination (TLI)
Heads of 0-24 hr old adult flies were detached and glued in an anterior up orientation to a microscope slide using a thin layer of clear nail polish. A drop of oil (Carl Zeiss Immersol, 518N) was placed on the sample and the eyes were examined under an upright light microscope (Zeiss Axiophot2). Shining a narrow bright beam of light from below the sample and optically neutralizing the cornea in an appropriate medium made the rhabdomeres visible (Franceschini and Kirschfeld, 1971a).

Immunohistochemistry
The retinas of 0-24 hr old adult flies were dissected in phosphate buffer (pH 7.4). The cornea and the rest of the head including the brain tissue were removed using forceps. Subsequently, the retinas were fixed in 4% formaldehyde in phosphate buffer (pH 7.4) for 15 min, followed by a 30 min wash in phosphate buffer (pH 7.4). Prior to antibody staining, the retinas were kept in a 0.3% Triton X-100 phosphate buffer solution at 4° for 24 hr or longer. The antibody staining was done according to a standard protocol. The following antibodies were used: rat anti-Crb (F3, 1:500; Pellikka *et al.*, 2002); mouse anti-Rh1 (4C5, 1:50; Developmental Studies Hybridoma Bank), guinea pig anti-Eys (G5, 1:500; Husain *et al.*, 2006), mouse anti-Nervana (nrv5f7, 1:50, Developmental Studies Hybridoma Bank), rabbit anti-GM130 (ab30637, 1:300, Abcam). Secondary antibodies anti-guinea pig alexa fluor 647 (A21450), anti-rat alexa fluor 555 (A21434), and anti-mouse alexa fluor 488 (A11029) were used at 1:400 (Molecular Probes/Thermo Fisher Scientific). Acti-stain555 (PHDG1-A, 1:75, Cytoskeleton Inc) was used to visualize rhabdomeres. A Leica TCS SP8 confocal microscope with 100x oil objective (NA 1.4) was used to capture images. Image J (Fiji) and Adobe Photoshop and Adobe Illustrator were used to edit and compile figures.

Electron Microscopy
Transmission electron microscopy (TEM) was performed on 0-24 hr old adult flies. Detached heads were bisected in ice-cold fixative solution (2% para-formaldehyde and 2.5% glutaraldehyde in 0.1 M sodium cacodylate, pH 7.4). The dissected tissue was kept in the above-mentioned
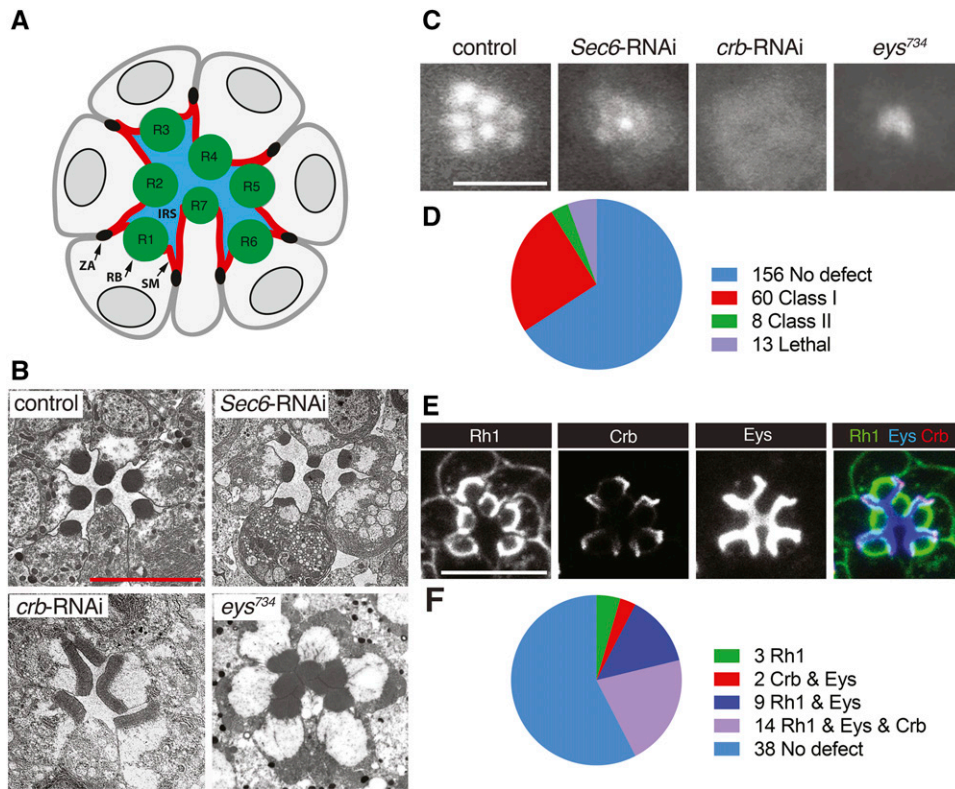
Figure 2 RNAi-based screen of known and predicted trafficking factors in *Drosophila* PRCs. GMR-GAL4 was used to drive the expression of UAS-dicer-2 and UAS-RNAi constructs. UAS-dicer-2/+; pGMR-Gal4/+ was used as control. Scale bars, 5 μm. (A) Schematic of cross-section of PRCs in a *Drosophila* ommatidium. Apical membranes of PRCs are subdivided into the rhabdomere (RB) and stalk membrane (SM). The stalk membrane connects the rhabdomere to the zonula adherens (ZA). PRCs R1-R8 (R8 is found below R7) surround the interrhabdomeral space (IRS). (B) TEM images of a wild-type, *Sec6*-RNAi, *crb*-RNAi, and eys⁷³⁴ mutant ommatidium. (C) TLI images of control, *Sec6*-RNAi, *crb*-RNAi, and eys⁷³⁴ mutant ommatidium. (D) Summary of the TLI screen. (E) Distribution of Rh1, Crb, and Eys in ommatidia of control flies. (F) Summary of data obtained from Rh1, Crb, and Eys retinal immunostaining of 66 Class I and Class II candidates identified with TLI (see also Figures S1-S4). Knockdown of 3 genes changed the distribution of Rh1, knockdown of 2 genes changed the distribution of both Crb and Eys, knockdown of 9 genes changed the distribution of both Rh1 and Eys, and knockdown of 14 genes changed the distribution of Rh1, Crb, and Eys.

fixative for 3 days at 4° on a nutator. Next, the tissue was washed with 0.1 M sodium cacodylate and treated with a solution of 1% osmium tetroxide and 0.1 M sorbitol in 0.1 M sodium cacodylate for 1 hr in the dark. After this treatment, the eyes were washed with 0.1 M sodium cacodylate and dehydrated in an ethanol series (50%, 70%, 80%, 100%) and embedded in Spurr's resin. Ultra-thin sections were stained with uranyl acetate and lead citrate. A Hitachi HT7000 transmission electron microscope was used to view the tissue at 700x magnification and an AMT XR-111 digital camera with AMT capture engine software (version 5.03) was used to capture images.

Interrhabdomeral space (IRS) quantification

Retinas were immuno-stained with anti-Eys antibody. Images were taken using a Leica TCS SP8 confocal microscope, with a 100x oil objective (NA 1.4). IRS size was then measured using Imaris software. Mean and standard deviation were calculated. An unpaired non-parametric Mann-Whitney test was performed to establish p values.

Stalk membrane quantification

Image J (Fiji) was used to measure stalk membranes from TEM images taken at 700x magnification. Individual stalk membranes were traced from the base of the rhabdomere to the zonula adherens and the length was measured. Mean and standard deviation were calculated. An unpaired non-parametric Mann-Whitney test was performed to establish p values.

Data availability

All data are included in the paper or the associated supplemental materials. All *Drosophila* stocks are available from public repositories.

All other reagents are commercially available or can be sent upon request. Supplemental material available at figshare: https://doi.org/10.25387/g3.10010408.

RESULTS AND DISCUSSION

Identification of genes involved in PRC vesicle trafficking

Drosophila PRCs are organized as elongated cylinders surrounding a lumen, the IRS, bound by PRC apical membranes (Figure 2A). PRCs deficient in Rh1, Eys, or Crb have prominent developmental defects. Rh1 is essential for rhabdomeral maintenance (Kumar and Ready 1995) and disruption of factors, such as the exocyt component Sec6 that affects the exocytosis of Rh1 and other rhabdomeral proteins show rhabdomeral deterioration (*e.g.*, Beronja *et al.*, 2005) (Figure 2B). The rhabdomeres of *crb* deficient PRCs appear enlarged and rectangular in cross-sections as a consequence of a distal to proximal extension defect (Pellikka *et al.*, 2002) (Figure 2B), and *eys* mutant ommatidia lack an IRS (Husain *et al.*, 2006; Zelhof *et al.*, 2006) (Figure 2B).

To identify factors associated with apical trafficking we screened RNAi lines targeting genes known or predicted to encode vesicle trafficking proteins for defects similar to Rh1, Crb, or Eys reduction. The eye-specific driver GMR-Gal4 (Freeman 1996) was used to express UAS-Dicer2 (to amplify the effects of RNAi; Ketting *et al.*, 2001) and a total of 309 RNAi lines corresponding to 237 genes (Table S1).

The first step in this screen was conducted using transmitted light illumination (TLI). TLI takes advantage of the fact that rhabdomeres act similar to optical fiber cables. When a beam of light is transmitted

■ **Table 1 Trafficking genes affecting Rh1, Crb, and Eys distribution in PRCs**

Cargo	Gene	CG #	RNAi line tested	Phenotype
Rh1	*Bet3*	*CG3911*	BDSC: 38302, VDRC: 21738	Cytoplasmic Rh1
	CdGAPr	*CG10538*	BDSC: 6437, 38279	Cytopslamic Rh1
	twf	*CG3172*	BDSC: 35365, 57375, VDRC: 25817	Cytoplasmic Rh1
Crb & Eys	*sqh*	*CG3595*	BDSC: 33892 & 32439	Larger IRS, longer Crb stained membrane, rectangular rhabdomeres for some ommatidia
	Rph	*CG11556*	BDSC: 25950, VDRC: 52438	Larger IRS, longer Crb stained membrane, rectangular rhabdomeres
Eys & Rh1	*Dhc64c*	*CG7507*	BDSC: 36698, 28749, 36583	Increase in cytoplasmic Rh1, cytoplasmic Eys and decrease in IRS size
	Khc	*CG7765*	BDSC: 25898, 35409	Cytoplasmic Rh1 and Eys
	Rab2	*CG3269*	BDSC: 28701, 34922, VDRC: 34767	Missing/smaller rhabdomeres and reduced IRS size
	Exocyst *Exo70 Exo84 Sec10 Sec15 Sec5 Sec6*	*CG7127 CG6095 CG6159 CG7034 CG8843 CG5341*	BDSC: 55234 BDSC: 28712 BDSC: 27483 BDSC: 27499 BDSC: 27526 VDRC:105836, 22079	Increase in cytoplasmic Rh1, cytoplasmic Eys and decrease in IRS size
Eys & Rh1 & Crb	*Chc*	*CG9012*	BDSC: 27530, VDRC: 23666	Reduced Crb, cytoplasmic Eys and Rh1
	aux	*CG1107*	BDSC: 35310, 39017	Reduced Crb, cytoplasmic Eys and Rh1
	shi	*CG18102*	BDSC: 36921, 28513	Cytoplasmic Eys, Crb, and Rh1 and retinal degeneration
	TSG101	*CG9712*	BDSC: 35710, VDRC: 23944	Cytoplasmic Rh1, smaller/ missing rhabdomeres, smaller IRS and less Crb
	Slh	*CG3539*	BDSC: 34335, 50940	Reduction of Rh1, Eys and Crb
	Shrb	*CG8055*	BDSC: 38305, VDRC: 106823	Cytoplasmic Eys, Crb, and Rh1 and retinal degeneration
	V-ATPase *Vha26 Vha100-1*	*CG1088 CG1709*	BDSC: 38996 BDSC: 26290	Cytoplasmic accumulation of Rh1, Crb and Eys
	Klc	*CG5433*	BDSC: 36795, 33934, 42597	Cytoplasmic Rh1 and Eys and reduction in Crb levels
	Rab1	*CG3320*	BDSC: 27299, VDRC: 330620	Reduction in Crb, Eys and Rh1
	Rab5	*CG3664*	BDSC: 30518, 34832	Many ommatidia disintegrated; less affected ommatidia had larger IRS, longer Crb stained stalks and degenerated rhabdomeres; reduced Rh1 at the rhabdomeres
	MyosinV	*CG2146*	VDRC: 16902 BDSC: 55740	Ectopic rhabdomeres at the basolateral membrane. Basolateral Eys and Crb. Cytoplasmic Rh1 and Eys.
	Avl/Syx7	*CG5081*	BDSC: 29546, VDRC:107264	Larger IRS, basolateral Rh1, longer Crb stained stalks
	Sec71	*CG7578*	BDSC: 32366, VDRC:100300	Significant reduction in Crb, Eys and Rh1, rhabdomeres absent

through the eye, individual rhabdomeres become visible, after the cornea has been optically neutralized in an appropriate medium (Franceschini and Kirschfeld, 1971a). Using TLI, 7 distinct rhabdomeres were visible in control flies (Figure 2C). Deviations from the control were categorized into 3 classes based on the severity and type of the defect. Mild to moderate rhabdomeral defects were categorized as class I. Here, one or more, but not all 7 rhabdomeres were distinguishable as individual entities. For example, the defect caused by *Sec6* knockdown would be categorized as class I (Figure 2C). Ommatidia where rhabdomeres appeared as a single diffuse patch were categorized as class II, as seen

for example with *crb* knockdown (Figure 2C). Rhabdomeres do exist in Crb deficient PRCs, but they transmit light poorly, likely as a result of their extension defect (Pellikka *et al.*, 2002). Finally, a class III phenotype showed an *eys*-like defect, where a single bright spot of light was visible per ommatidium (Figure 2C), as a result of a loss of the IRS (Husain *et al.*, 2006; Zelhof *et al.*, 2006).

Figure 2D summarizes the results of the TLI screen. Out of the 237 genes screened, we found that the knockdown of 68 genes produced a class I or II defect. We did not observe a class III defect. This suggested that among the trafficking genes tested, no factor exclusively
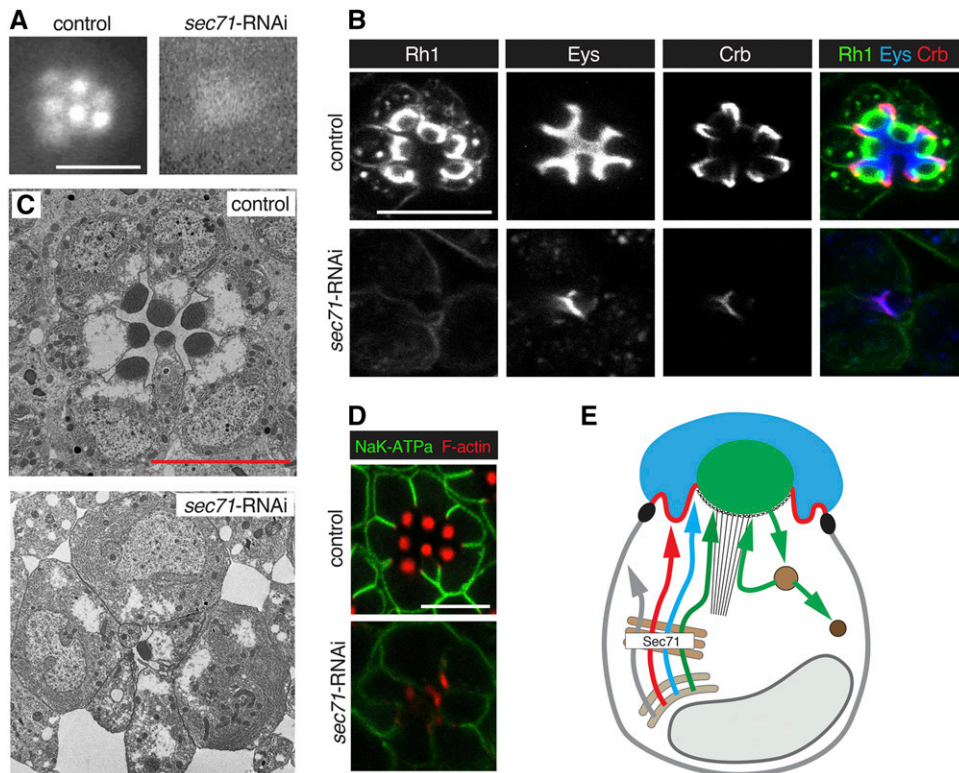
Figure 3 Knockdown of *Sec71* caused a reduction of both apical and basolateral proteins. RNAi line BDSC 32366 (*Sec71*-RNAi) was used. Flies with *Sec71*-RNAi were crossed to UAS-dicer-2; pGMR-Gal4. UAS-dicer-2/+; pGMR-Gal4/+ was used as control. Scale bars are 5 μm. (A) TLI does not reveal individual rhabdomeres in *Sec71* knockdown PRCs (Class II defect). (B) *Sec71* deficient PRCs show a severe reduction of Rh1, Crb, and Eys. (C) TEM shows a loss of IRS, missing rhabdomeres and gaps between ommatidial units of Sec71 deficient PRCs. (D) The K+Na+ATPase subunit Nrv is reduced in *Sec71* knockdown PRCs. Acti-stain555 (F-actin) was used to visualize the rhabdomeres. (E) Summary model suggesting that Sec71 acts in the Golgi to control secretion of apical and basolateral factors. See Figure 1A for annotation and text for discussion.

compromises Eys trafficking without affecting also other apical proteins. Additionally, 13 genotypes were associated with lethality, indicating a leaky expression of the RNAi construct in essential tissues.

RNAi knockdown causing a class I or II defect were further analyzed through immunostaining of retinas for Rh1, Crb, and Eys (Figure 2E). Two phenotypes that were not further analyzed were caused by *Rab11* and *Rab21* knockdown as depletion of these genes led to fragile eye tissue that fell apart during dissection. Out of the 66 genes examined, we found that the knockdown of 28 genes changed the amount and/or localization of one or more apical proteins (Figure 2F and Table 1). 21 of our hits were confirmed with a second independent RNAi line. Seven genes were not tested with a second RNAi line as they encoded multiple components of two protein complexes (the exocyst and the V-ATPase) that were associated with similar defects in protein distribution (Tables 1 and S1). We did not find genes that have an exclusive effect on Eys or Crb. We also did not find a case where Crb and Rh1 trafficking was affected in the absence of changes to Eys.

We performed a more in-depth analysis of the defects caused by loss of Sec71 (Figure 3), exocyst (Figure 4), dynein (Figure 5) and Syx7/Avl (Figure 6). We selected these factors as their knockdown was associated with robust defects, and as they represented a component of the Golgi (Sec71), secretory (exocyst and dynein), and the endocytic (Syx7/Avl) pathways. Defects caused by the knockdown of other factors can be found in Figure S1 (for RNAi constructs affecting Rh1), Figure S2 (for RNAi constructs affecting Rh1 and Eys), Figure S3 (for RNAi constructs affecting Crb and Eys), and Figure S4 (for RNAi constructs affecting all three apical proteins).

Sec71 is required for biosynthetic traffic of both apical and basolateral proteins

The Arf GEF Sec71 is essential for the integrity of Golgi compartments in *Drosophila* ddaC sensory neurons (Wang *et al.*, 2017). The function of

Sec71 in PRCs was unknown. The expression of two different *Sec71* RNAi lines led to a class II defect as seen with TLI (Figure 3A). We observed a robust reduction but normal distribution of Eys, Crb, and Rh1 (Figure 3B). *Sec71* knockdown affected the integrity and survival of cells in the retina as ultrastructural analysis showed retinal holes, dying and/or absent PRCs, and small or missing rhabdomeres (Figure 3C).

A similar reduction in Eys, Crb, and Rh1 amounts were also observed in Rab1 deficient PRCs (Figure S4). Rab1 has been associated with the ER to Golgi trafficking of Rh1 (Satoh *et al.*, 1997). Proper processing at the Golgi is thought to be important for protein stability, and disruption of factors required for ER to Golgi processing such as Syx5 and Rab1 are known to cause an overall reduction in cargo levels (Satoh *et al.*, 2016, Satoh *et al.*, 1997). Therefore, the reduction of Eys, Crb, and Rh1 seen in Sec71 compromised PRCs may be due to a lack of Golgi processing, suggesting a role for Sec71 at or prior to the Golgi in the biosynthetic pathway.

This conclusion is further supported by our observations that also the basolateral protein Nervana (Nrv), a subunit of the Na+/K+ ATPase was reduced in *Sec71* knockdown PRCs (Figure 3D). This suggests that Sec71 acts prior to the separation of apical and basolateral trafficking routes, which is thought to occur at or prior to the *trans*-Golgi network (TGN). Similar defects in apical and basolateral protein transport have been described for the Golgi-associated SNARE protein Syx5 (Satoh *et al.* 2016). Taken together, our observations indicate that Sec71 contributes to the secretion of both apical and basolateral proteins in PRCs, suggesting a defect in Golgi processing (Figure 3E).

Sec71 is related to the human Arf GEF BIG1/BIG2 family (Christis and Munro 2012). BIG1 and BIG2 are associated with the TGN (Mansour *et al.*, 1999; Yamaji *et al.*, 2000; Shinotsuka *et al.*, 2002; Zhao *et al.*, 2002; Ishizaki *et al.*, 2008), and the recycling endosomes (Shin *et al.*, 2004; Shen *et al.*, 2006; Ishizaki *et al.*,
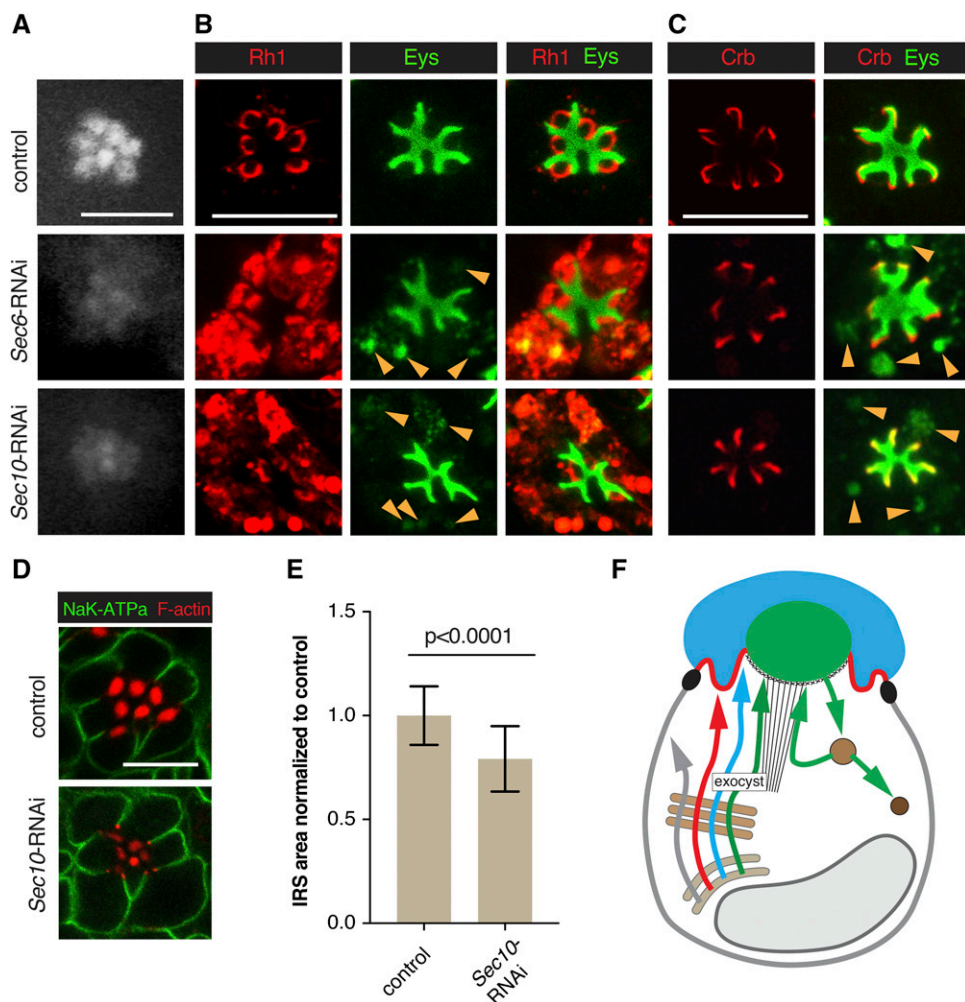
Figure 4 The exocyst contributes to Rh1 and Eys exocytosis. RNAi line VDRC 22079 (*Sec6*-RNAi) was used to knock down Sec6, and line BDSC 27483 (*Sec10*-RNAi) to deplete Sec10. *Sec6*-RNAi or *Sec10*-RNAi were crossed with UAS-dicer-2; pGMR-Gal4. UAS-dicer-2/+; pGMR-Gal4/+ was used as control. Scale bars, 5 μm. (A) Individual rhabdomeres were only partially visible in Sec6 and Sec10 deficient retinas using TLI. Both were categorized as Class I. (B) Sec6 and Sec10 deficient PRCs show cytoplasmic accumulation of Rh1 and Eys (arrowheads). Cytoplasmic Eys colocalizes with Rh1. (C) No defect was observed for Crb levels or localization in exocyst knockdown PRCs. Cytoplasmic Eys in exocyst deficient PRCs is visible in the absence of Rh1 staining (arrowheads), eliminating the possibility of cross-reaction between Eys and Rh1 antibodies as an explanation for the cytoplasmic Eys signal seen in (B). (D) Levels/localization of the basolateral protein Nrv (K$^+$Na$^+$ATPase subunit) was not affected in exocyst compromised PRCs. Acti-stain555 (F-actin) was used to visualize the rhabdomeres. (E) IRS size was significantly reduced in *Sec10* deficient retinas. A total of 69 individual IRS were measured for control and 118 for *Sec10* RNAi ommatidia, using three different animals per genotype. Values were normalized to the control. Error bars represent standard deviation. Unpaired non-parametric Mann-Whitney test. (F) Summary model indicating the secretion of Rh1 and Eys containing secretory vesicles depends on the exocyst. See Figure 1A for annotation and text for discussion.

2008). In *Drosophila* sensory neurons, Sec71 is mainly found at the TGN, and the Golgi is severely disrupted in Sec71-deficient cells (Wang *et al.*, 2017).

As an Arf GEF, Sec71 is likely to activate one or more resident Golgi Arfs in PRCs. Candidates to consider are Arf1, Arf4, and Arl1. Arf1 (Arf79F in *Drosophila*), is important in regulating traffic at the Golgi apparatus (Rodrigues and Harris 2017). In sensory neurons, Sec71 activates Arf1, and the Golgi apparatus is disrupted in *Arf1* mutant cells (Wang *et al.*, 2017). Arf4 (Arf102F in *Drosophila*), is associated with the TGN and is important in targeting rhodopsin to the cilia of frog PRCs (Mazelova *et al.*, 2009; Wang *et al.*, 2012). Finally, Arl1 (Arf72A in *Drosophila*), localizes to the Golgi in *Drosophila* PRCs and is important in quality assurance of cargo proteins (Lee *et al.*, 2011). Loss of Arl1 results in an increase of Golgi compartments and an acceleration of Rh1 secretion (Lee *et al.*, 2011). In our TLI screen, Arf4 RNAi caused lethality, whereas the expression of Arf1 and Arl1 RNAi lines did not show an effect. This may be due to the inactivity/low activity of the RNAi lines used, or functional redundancies between Arfs in PRCs.

The exocyst complex contributes to both Rh1 and Eys secretion

Depletion of exocyst components Exo70, Exo84, Sec10, Sec15, Sec5 and Sec6 led to class I defects (see Figure 4A for Sec6 and Sec10 data). Rhabdomeral defects were expected as the exocyst is known to be important for the exocytosis of rhabdomeral proteins (Beronja *et al.*, 2005). As previously described for *Sec6* mutant PRCs (Beronja *et al.*, 2005), we observed cytoplasmic accumulation of Rh1 in *Sec6* and *Sec10* knockdown PRCs (Figure 4B), smaller rhabdomeres, and a cytosolic accumulation of secretory vesicles (Figure 2B).

Unexpectedly, in addition to Rh1 trafficking defects, we also noted cytoplasmic Eys for all exocyst RNAi lines tested (see Figure 4B and C). Cytoplasmic Eys and Rh1 partially overlapped with all cytoplasmic Eys accumulations also highly enriched in Rh1, suggesting that Eys and Rh1 are trapped in the same cytoplasmic compartments in exocyst deficient PRCs (Figure 4B). Expression of several exocyst RNAi constructs also resulted in a smaller than normal IRS (Figure 4B). We quantified the size of the Eys-positive area in Sec10-depleted PRCs in comparison to control ommatidia and found that the IRS size was
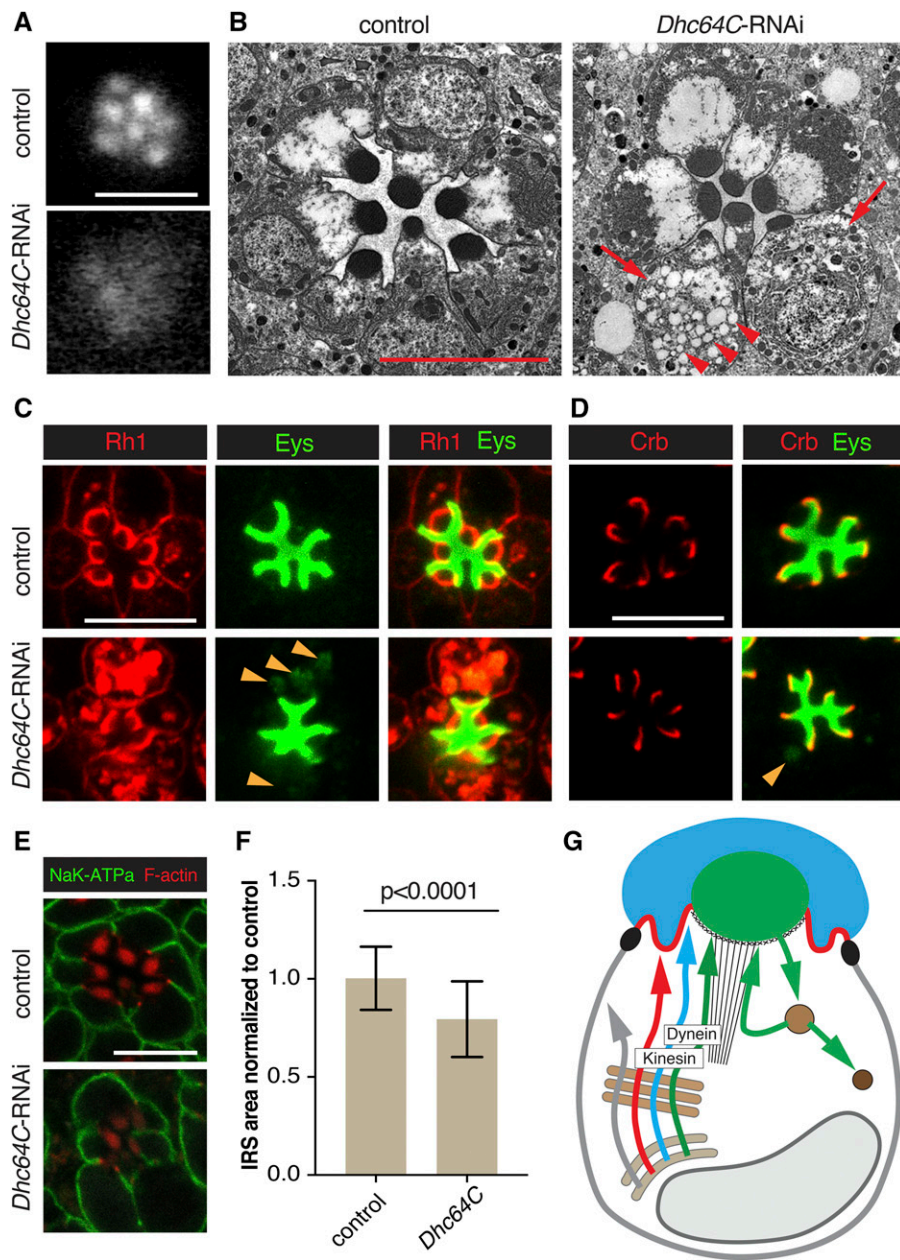
Figure 5 Dynein is important for Rh1 and Eys trafficking. RNAi line BDSC 36583 (*Dhc64C*-RNAi) was used to deplete Dhc64c. *Dhc64C*-RNAi was crossed with UAS-dicer-2; pGMR-Gal4. UAS-dicer-2/+; pGMR-Gal4/+ was used as control. Scale bars, 5 μm. (A) Individual rhabdomeres were partially visible in dynein (Dhc64c) deficient retinas. We categorized this defect as Class I. (B) TEM analysis revealed a smaller IRS, smaller rhabdomeres, bloated PRCs (arrow) and cytoplasmic accumulation of vesicles (arrowheads) in dynein deficient retinas. (C) Dynein deficient PRCs showed cytoplasmic accumulation of Rh1 and Eys (arrowheads). Cytoplasmic Eys colocalized with cytoplasmic Rh1. (D) Levels or localization of Crb was normal in Dhc64c depleted PRCs. Arrowhead points to cytoplasmic accumulation of Eys. (E) Levels/localization of the basolateral protein Nrv (K⁺Na⁺ATPase subunit) was not affected by dynein depletion. Acti-stain555 (F-actin) was used to visualize the rhabdomeres. (F) IRS size was significantly reduced in dynein compromised retinas. A total of 106 individual IRS were measured for control and 109 for dynein deficient ommatidia using 3 different animals per genotype. Values were normalized to the control. Error bars represent standard deviation. Unpaired nonparametric Mann-Whitney test. (G) Summary model indicating the secretion of Rh1 and Eys containing secretory vesicles depends on dynein and that secretion of Rh1, Eys, and Crb requires kinesin function (see Figures S2 and S4). See Figure 1A for annotation and text for discussion.

reduced by ~20% (Figure 4E). As IRS size is dependent on Eys levels (Husain *et al.*, 2006; Zelhof *et al.*, 2006), it is likely that the IRS is reduced due to ineffective Eys trafficking. We did not observe a noticeable change in Crb (Figure 4C) or basolateral trafficking of Nrv (Figure 4D).

It was previously thought that Eys was secreted through the stalk membrane and would not be affected by defects in rhabdomeral trafficking (Husain *et al.*, 2006). The different impact on Eys trafficking observed here compared to our previous analysis may be the result of the different strategies used to compromise exocyst function (RNAi used here *vs.* generation of *Sec6* mutant clones combined with the expression of a partial rescue construct to avoid cell lethality caused by the loss of exocyst function; Beronja *et al.*, 2005; Husain *et al.*, 2006). We conclude that the exocyst complex, which is crucial for trafficking to the rhabdomere, is also important for Eys trafficking to the IRS (Figure 4F).

Microtubule motor protein dynein is required for Rh1 and Eys secretion

The function of dynein, a minus-end directed microtubule motor protein, has not been previously described in fly PRCs. We observed class I defects with three distinct RNAi lines targeting Dynein heavy chain 64C (Dhc64C) (Figure 5A). We observed abnormal cytoplasmic accumulation of Rh1 and Eys for all three RNAi lines (Figure 5C and D). The presence of cytoplasmic Eys partially overlapped with Rh1, suggesting that Eys and Rh1 are trapped in the same compartments. Cytoplasmic Eys was coupled with a reduction in IRS size (Figure 5F). We did not observe an effect on Crb (Figure 5D) or basolateral Nrv (Figure 5E), suggesting that traffic to the stalk and the basolateral membrane was not affected.

Expanded cell bodies and an accumulation of cytoplasmic vesicles of various sizes are apparent in Dhc64C depleted PRCs (Figure 5B). These vesicles looked similar to the secretory vesicles described for PRCs
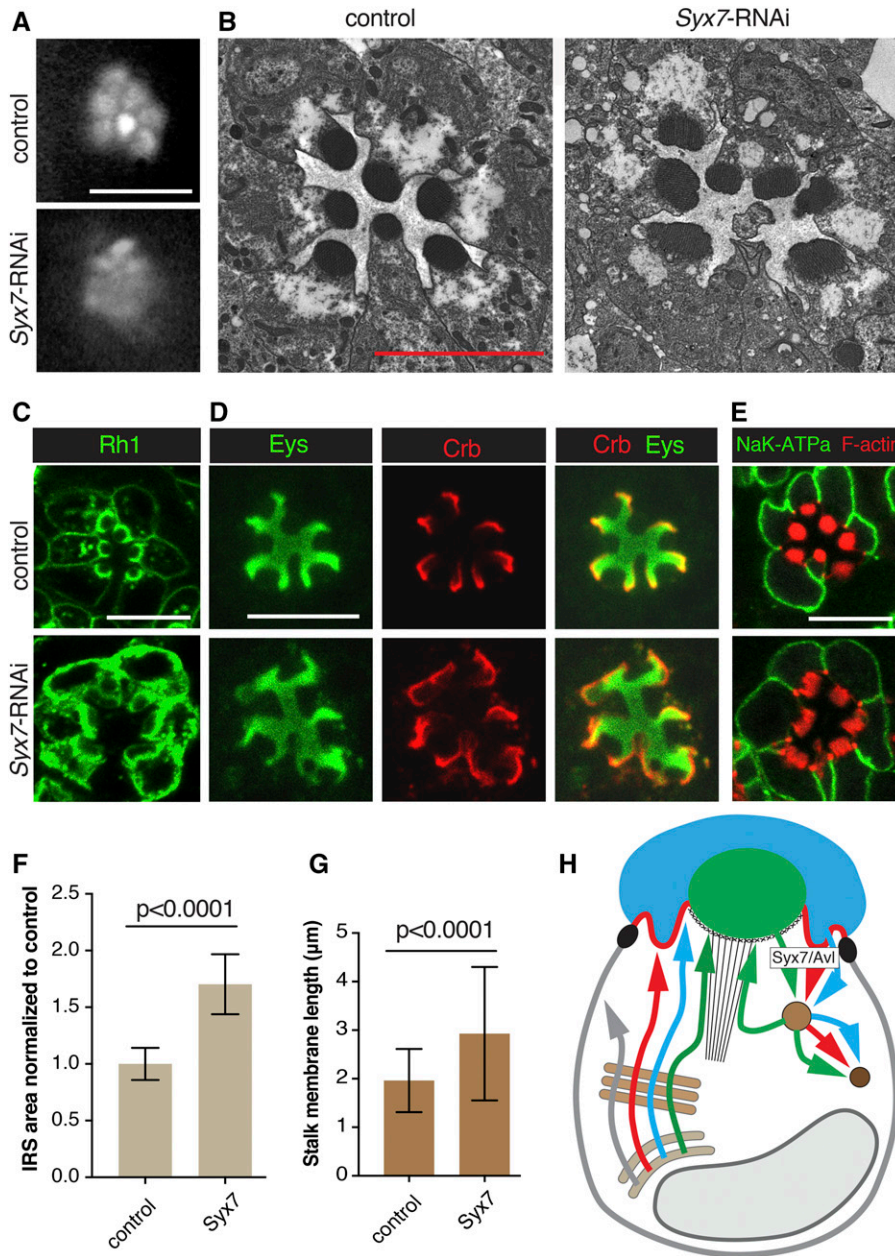
Figure 6 Syx7/Avl deficient PRCs show enhanced surface levels of Rh1, Eys and Crb. RNAi line BDSC 29546 (*Syx7*-RNAi) was used to deplete Syx7/Avl. *Syx7*-RNAi was crossed with UAS-dicer-2; pGMR-Gal4. UAS-dicer-2/+; pGMR-Gal4/+ was used as control. Scale bars, 5 μm. (A) Individual rhabdomeres were partially visible in Syx7/Avl deficient retinas. We categorized this defect as Class I. (B) Knockdown of Syx7/*Avl* led to rhabdomeral fragmentation and degeneration. (C) Syx7/Avl deficient PRCs show increased apical and basolateral accumulation of Rh1. (D) IRS area stained with Eys and stalk membranes labeled with Crb are larger in Syx7/Avl deficient PRCs compared to the control. (E) Levels/localization of the basolateral protein Nrv (K^+Na^+ ATPase subunit) is normal in Syx7/Avl deficient PRCs. Acti-stain555 (F-actin) was used to visualize rhabdomeres which appear disorganized. (F) IRS size was significantly larger in Syx7/Avl deficient retinas compared to controls. A total of 69 individual IRS were measured for the control and 138 for Syx7/*Avl* knockdown PRCs using 3 different animals per genotype. Values were normalized to the control. Error bars represent standard deviation. Unpaired non-parametric Mann-Whitney test. (G) Stalk membranes were significantly larger in Syx7-Avl deficient PRCs compared to controls. A total of 182 individual stalk membranes were measured for the control and 126 for Syx7/Avl deficient knockdown PRCs. Error bars represent standard deviation. Unpaired non-parametric Mann-Whitney test. (H) Summary model indicating that the endocytosis of Rh1, Crb, and Eys depends on Syx7/Avl. See Figure 1A for annotation and text for discussion.

compromised for the exocyst, Rab11, Rip11, or Myosin V (Satoh *et al.*, 2005; Beronja *et al.*, 2005; Li *et al.*, 2007). Notably, we also observed similar defects with the microtubule plus-end directed kinesin motor. Depletion of Kinesin heavy chain (Khc) and Kinesin light chain (Klc) led to a Class I defect in TLI. Rh1 and Eys accumulated in the cytoplasm and IRS size was decreased (Figure S2 and S4). It is curious that the knockdown of both plus-end and minus-end directed motors caused similar Eys and Rh1 secretion defects.

Klc-deficient PRCs (but not Khc-deficient cells) also showed a reduction in Crb (Figure S4). Microtubules and microtubule-related proteins are known to be important for Crb trafficking in pupal PRCs (Mukhopadhyay *et al.*, 2010; Chen *et al.*, 2010; League and Nam 2011; Mui *et al.*, 2011; Nam 2016). It is not clear whether this Crb defect is specific to Klc knockdown or if a stronger knockdown of Khc or Dhc64C would affect Crb in a similar manner.

Previous studies in the developing eye discs showed that the plus-end of microtubules are found at the apical cell membrane whereas the minus-ends are located in the vicinity of the cell nucleus (Mosley-Bishop *et al.* 1999). Microtubule orientation in adult PRCs is not known and would be important to address in future studies to help in the interpretation of defects resulting from knockdown of motor proteins. Vertebrate PRCs possess microtubules with opposing orientations (for review see Nemet *et al.*, 2015) Rhodopsin is made in the inner segment (IS) of vertebrate PRCs and transported to the vertebrate equivalent of the rhabdomere, the outer segment (OS). Within the IS, microtubules are orientated with their plus-ends at the Golgi and minus-ends at the base of the OS. Microtubule orientation is reversed in the OS, where the minus-end is found at the base of the OS, while the plus-end is found at the distal end of the OS. It has been proposed that dynein is important in the trafficking of rhodopsin from Golgi to the OS, whereas kinesin is important in trafficking from the base of the OS to its tip

(Nemet *et al.*, 2015). Loss of dynein or kinesin function may therefore lead to defects in rhodopsin trafficking.

Taken together, we found that microtubule motors, kinesin and dynein are essential in the secretion of Eys and Rh1. One important conclusion from our findings is that microtubule and actin-based transport mechanisms cooperate in the delivery of rhabdomere-targeted proteins. Previous studies had revealed the importance of actin filament-based routes and the actin motor protein Myosin V in rhabdomeral vesicle trafficking (Li., *et al.*, 2007). It would be interesting to examine how microtubule and actin-based transport mechanisms interface to facilitate apical trafficking in *Drosophila* PRCs.

Syntaxin 7/Avalanche is required for Rh1, Eys, and Crb endocytosis

Syx7/Avl is required for apical endocytosis in imaginal disc epithelia. Syx7/Avl deficient cells displayed an excessive accumulation of Crb at the apical membrane (Lu and Bilder 2005). Syx7/Avl co-localizes with Rab5 and is required for the entry of cargo proteins, such as Crb into early endosomes (Lu and Bilder 2005). Previous results suggested that endocytosis is essential for rhabdomeral maintenance in *Drosophila* PRCs. Endocytosis is thought to be important in the proper formation of the interface between the rhabdomere and the sub-rhabdomeric space where the rhabdomere terminal web in located (Pinal and Pichaud 2011). Here, we found that knockdown of Syx7/Avl using two distinct RNAi lines led to a class I defect with TLI (Figure 6A), and consistent with earlier results indicating that endocytosis promotes rhabdomere integrity, we observed structural defects in rhabdomeres of Syx7/Avl knockdown PRCs (Figure 6B and E).

Rh1, Crb, and Eys levels were increased in Syx7/Avl compromised PRCs whereas Nrv levels remained normal (Figure 6C, D and E). Corresponding to the increase in Eys (Zelhof *et al.*, 2006) we found an enlarged IRS in Syx7/Avl knockdown PRCs (Figure 6F). Similarly, the overabundance of Crb in Syx7/Avl knockdown PRCs was associated with an enlarged stalk membrane (Figure 6G) as previously reported for PRCs that overexpress Crb (Pellikka *et al.*, 2002). The apical accumulation of Eys and Crb as a result of compromised apical endocytosis suggests that both proteins similar as Rh1 undergo active turnover in *Drosophila* PRCs.

Interestingly, Rh1 was increased not only at the apical rhabdomere but also at the basolateral membrane in Syx7/Avl knockdown PRCs, where in control PRCs only small amounts of Rh1 are found (Figure 6C). It is possible that an over-accumulation of Rh1 at the rhabdomeres led to a leakage of Rh1 into the basolateral membrane. Alternatively, it is possible that at least some Rh1 may normally be transcytosed from the basolateral to the apical membrane, requiring basolateral endocytosis. As we did not find an effect on the basolateral protein Nrv (Figure 6E) we favor the first possibility, and would predict that Syx7/Avl is associated with the apical membrane of PRCs.

Concluding remarks

By exploring apical vesicle trafficking in the fly PRCs through an RNAi-based screen we have uncovered 28 genes involved in apical localization of the key PRC proteins Rh1, Crb, and Eys. We have shown that the Arf GEF Sec71 is essential for proper apical and basolateral protein trafficking, the exocyst complex and microtubule motors dynein and kinesin are important for Eys and Rh1 secretion, and the syntaxin Syx7/Avl is involved in Crb, Eys, and Rh1 endocytosis. Our results have implications for the understanding of human eye diseases as mutations in human orthologs of Eys, Crb, and Rh1 cause eye degenerative diseases (Abd El-Aziz *et al.*, 2008; Collin *et al.*, 2008; Richard *et al.*, 2006; den Hollander *et al.*, 2008; Hollingsworth and Gross 2012). The rhabdomere

and the stalk membrane in *Drosophila* correspond topologically and functionally to the vertebrate rod and cone outer segment and inner segment, respectively. It is likely that similar factors are involved in apical trafficking in *Drosophila* and vertebrate PRCs. One example is Rab11, which was shown to be important in post-Golgi Rh1 exocytosis in both *Drosophila* and vertebrates (Satoh *et al.*, 2005; Mazelova *et al.*, 2009). It will therefore be of interest to further explore the conservation of vesicle trafficking mechanisms in *Drosophila* and mammalian PRCs.

LITERATURE CITED

Abd El-Aziz, M. M., I. Barragan, C. A. O'Driscoll, L. Goodstadt, E. Prigmore *et al.*, 2008 EYS, encoding an ortholog of *Drosophila* spacemaker, is mutated in autosomal recessive retinitis pigmentosa. Nat. Genet. 40: 1285–1287. https://doi.org/10.1038/ng.241

Alloway, P. G., L. Howard, and P. J. Dolph, 2000 The formation of stable rhodopsin-arrestin complexes induces apoptosis and photoreceptor cell degeneration. Neuron 28: 129–138. https://doi.org/10.1016/S0896-6273(00)00091-X

Beronja, S., P. Laprise, O. Papoulas, M. Pellikka, J. Sisson *et al.*, 2005 Essential function of *Drosophila* Sec6 in apical exocytosis of epithelial photoreceptor cells. J. Cell Biol. 169: 635–646. https://doi.org/10.1083/jcb.200410081

Bujakowska, K., I. Audo, S. Mohand-Saïd, M. E. Lancelot, A. Antonio *et al.*, 2012 CRB1 mutations in inherited retinal dystrophies. Hum. Mutat. 33: 306–315. https://doi.org/10.1002/humu.21653

Chen, G., G. P. League, and S. C. Nam, 2010 Role of spastin in apical domain control along the rhabdomere elongation in *Drosophila* photoreceptor. PLoS One 5: e9480. https://doi.org/10.1371/journal.pone.0009480

Chinchore, Y., A. Mitra, and P. J. Dolph, 2009 Accumulation of rhodopsin in late endosomes triggers photoreceptor cell degeneration. PLoS Genet. 5: e1000377. https://doi.org/10.1371/journal.pgen.1000377

Christis, C., and S. Munro, 2012 The small G protein Arl1 directs the trans-Golgi-specific targeting of the Arf1 exchange factors BIG1 and BIG2. J. Cell Biol. 196: 327–335. https://doi.org/10.1083/jcb.201107115

Colley, N. J., J. A. Cassill, E. K. Baker, and C. S. Zuker, 1995 Defective intracellular transport is the molecular basis of rhodopsin-dependent dominant retinal degeneration. Proc. Natl. Acad. Sci. USA 92: 3070–3074. https://doi.org/10.1073/pnas.92.7.3070

Collin, R. W., K. W. Littink, B. J. Klevering, L. I. van den Born, R. K. Koenekoop *et al.*, 2008 Identification of a 2 Mb human ortholog of *Drosophila* eyes shut/spacemaker that is mutated in patients with retinitis pigmentosa. Am. J. Hum. Genet. 83: 594–603. https://doi.org/10.1016/j.ajhg.2008.10.014

den Hollander, A. I., J. B. ten Brink, Y. J. de Kok, S. van Soest, L. I. van den Born *et al.*, 1999 Mutations in a human homologue of *Drosophila* crumbs cause retinitis pigmentosa (RP12). Nat. Genet. 23: 217–221. https://doi.org/10.1038/13848

den Hollander, A. I., R. Roepman, R. K. Koenekoop, and F. P. Cremers, 2008 Leber congenital amaurosis: genes, proteins and disease mechanisms. Prog. Retin. Eye Res. 27: 391–419. https://doi.org/10.1016/j.preteyeres.2008.05.003

Franceschini, N., and K. Kirschfeld, 1971a In vivo optical study of photoreceptor elements in the compound eye of *Drosophila*. Kybernetik 8: 1–13. https://doi.org/10.1007/BF00270828

Freeman, M., 1996   Reiterative use of the EGF receptor triggers differenti-ation of all cell types in the *Drosophila* eye. Cell 87: 651–660. https://doi.org/10.1016/S0092-8674(00)81385-9

Hollingsworth, T. J., and A. K. Gross, 2012   Defective trafficking of rho-dopsin and its role in retinal degenerations. Int. Rev. Cell Mol. Biol. 293: 1–44. https://doi.org/10.1016/B978-0-12-394304-0.00006-3

Husain, N., M. Pellikka, H. Hong, T. Klimentova, K. M. Choe et al., 2006   The Agrin/Perlecan-Related Protein Eyes Shut is Essential for Epithelial Lumen Formation in the *Drosophila* Retina. Dev. Cell 11: 483–493. https://doi.org/10.1016/j.devcel.2006.08.012

Ishizaki, R., H. W. Shin, H. Mitsuhashi, and K. Nakayama, 2008   Redundant roles of BIG2 and BIG1, guanine-nucleotide exchange factors for ADP-ribosylation factors in membrane traf c between the trans-Golgi network and endosomes. Mol. Biol. Cell 19: 2650–2660. https://doi.org/10.1091/mbc.e07-10-1067

Iwanami, N., Y. Nakamuram, T. Satoh, Z. Liu, and A. K. Satoh, 2016   Rab6 is required for multiple apical transport pathways but not the basolateral transport pathway in *Drosophila* photoreceptors. PLoS Genet. 12: e1005828. https://doi.org/10.1371/journal.pgen.1005828

Izaddoost, S., S. C. Nam, M. A. Bhat, H. J. Bellen, and K. W. Choi, 2002   *Drosophila* Crumbs is a positional cue in photoreceptor adherens junctions and rhabdomers. Nature 416: 178–183. https://doi.org/10.1038/nature720

Johnson, K., F. Grawe, N. Grzeschik, and E. Knust, 2002   *Drosophila* crumbs is required to inhibit light-induced photoreceptor degeneration. Curr. Biol. 12: 1675–1680. https://doi.org/10.1016/S0960-9822(02)01180-6

Ketting, R., S. E. Fischer, E. Bernstein, T. Sijen, G. J. Hannon et al., 2001   Dicer functions in RNA interference and in synthesis of small RNA involved in developmental timing in *C. elegans*. Genes Dev. 15: 2654–2659. https://doi.org/10.1101/gad.927801

Kiselev, A., M. Socolich, J. Vinós, R. W. Hardy, C. S. Zuker et al., 2000   A molecular pathway for light-dependent photoreceptor apoptosis in *Drosophila*. Neuron 28: 139–152. https://doi.org/10.1016/S0896-6273(00)00092-1

Kumar, J. P., and D. F. Ready, 1995   Rhodopsin plays an essential structural role in *Drosophila* photoreceptor development. Development 121: 4359–4370.

League, G. P., and S. C. Nam, 2011   Role of kinesin heavy chain in Crumbs localization along the rhabdomere elongation in *Drosophila* photore-ceptor. PLoS One 6: e21218. https://doi.org/10.1371/journal.pone.0021218

Lee, J., J. Lee, and B. G. Ju, 2011   *Drosophila* Arf72A acts as an essential regulator of endoplasmic reticulum quality control and suppresses autosomal-dominant retinopathy. Int. J. Biochem. Cell Biol. 43: 1392–1401. https://doi.org/10.1016/j.biocel.2011.06.004

Li, B. X., A. K. Satoh, and D. F. Ready, 2007   Myosin V, Rab11, and dRip11 direct apical secretion and cellular morphogenesis in developing *Drosophila* photoreceptors. J. Cell Biol. 177: 659–669. https://doi.org/10.1083/jcb.200610157

Lu, H., and D. Bilder, 2005   Endocytic control of epithelial polarity and proliferation in *Drosophila*. Nat. Cell Biol. 7: 1232–1239. https://doi.org/10.1038/ncb1324

Mansour, S. J., J. Skaug, X. H. Zhao, J. Giordano, S. W. Scherer et al., 1999   p200 ARF-GEP1: a Golgi-localized guanine nucleotide exchange protein whose Sec7 domain is targeted by the drug brefeldin. A. Proc. Natl. Acad. Sci. **96**: 7968–7973. https://doi.org/10.1073/pnas.96.14.7968

Mazelova, J., L. Astuto-Gribble, H. Inoue, B. M. Tam, E. Schonteich et al., 2009   Ciliary targeting motif VxPx directs assembly of a trafficking module through Arf4. EMBO J. 28: 183–192. https://doi.org/10.1038/emboj.2008.267

Mosley-Bishop, K. L., Q. Li, L. Patterson, and J. A. Fischer, 1999   Molecular analysis of the klarsicht gene and its role in nuclear migration within differentiating cells of the *Drosophila* eye. Curr. Biol. 9: 1211–1220. https://doi.org/10.1016/S0960-9822(99)80501-6

Mui, U. N., C. M. Lubczyk, and S. C. Nam, 2011   Role of spectraplakin in *Drosophila* photoreceptor morphogenesis. PLoS One 6: e25965. https://doi.org/10.1371/journal.pone.0025965

Mukhopadhyay, B., S. C. Nam, and K. W. Choi, 2010   Kinesin II is required for cell survival and adherens junction positioning in *Drosophila* photo-receptors. Genesis 48: 522–530. https://doi.org/10.1002/dvg.20642

Nam, S. C., 2016   Role of Tau, a microtubule associated protein, in *Drosophila* photoreceptor morphogenesis. Genesis 54: 553–561. https://doi.org/10.1002/dvg.22966

Nemet, I., P. Ropelewski, and Y. Imanishi, 2015   Rhodopsin Trafficking and Mistrafficking: Signals, Molecular Components, and Mechanisms. Prog. Mol. Biol. Transl. Sci. 132: 39–71. https://doi.org/10.1016/bs.pmbts.2015.02.007

Pellikka, M., G. Tanentzapf, M. Pinto, C. Smith, G. J. McGlade et al., 2002   Crumbs, the *Drosophila* homologue of human CRB1/RP12, is essential for photoreceptor morphogenesis. Nature 416: 143–149. https://doi.org/10.1038/nature721

Pellikka, M., and U. Tepass, 2017   Unique cell biological profiles of retinal disease-causing missense mutations in the polarity protein Crumbs. J. Cell Sci. 130: 2147–2158. https://doi.org/10.1242/jcs.197178

Pinal, N., and F. Pichaud, 2011   Dynamin- and Rab5-dependent endocytosis is required to prevent *Drosophila* photoreceptor degeneration. J. Cell Sci. 124: 1564–1570. https://doi.org/10.1242/jcs.082115

Pocha, S. M., A. Shevchenko, and E. Knust, 2011   Crumbs regulates rho-dopsin transport by interacting with and stabilizing myosin V. J. Cell Biol. 195: 827–838. https://doi.org/10.1083/jcb.201105144

Richard, M., R. Roepman, W. M. Aartsen, A. G. van Rossum, A. I. den Hollander et al., 2006   Towards understanding CRUMBS function in retinal dystrophies. Hum. Mol. Genet. 15: R235–R243. https://doi.org/10.1093/hmg/ddl195

Rodrigues, F. F., and T. J. Harris, 2017   Key roles of Arf small G proteins and biosynthetic trafficking for animal development. Small GTPases. https://doi.org/10.1080/21541248.2017.1304854

Satoh, A., F. Tokunaga, S. Kawamura, and K. Ozaki, 1997   In situ inhibition of vesicle transport and protein processing in the dominant negative Rab1 mutant of *Drosophila*. J. Cell Sci. 110: 2943–2953.

Satoh, A. K., J. E. O'Tousa, K. Ozaki, and D. F. Ready, 2005   Rab11 mediates post-Golgi trafficking of rhodopsin to the photosensitive apical mem-brane of *Drosophila* photoreceptors. Development 132: 1487–1497. https://doi.org/10.1242/dev.01704

Satoh, T., Y. Nakamura, and A. K. Satoh, 2016   The roles of Syx5 in Golgi morphology and Rhodopsin transport in *Drosophila* photoreceptors. Biol. Open 5: 1420–1430. https://doi.org/10.1242/bio.020958

Schopf, K., and A. Huber, 2017   Membrane protein trafficking in *Drosophila* photoreceptor cells. Eur. J. Cell Biol. 96: 391–401. https://doi.org/10.1016/j.ejcb.2016.11.002

Shen, X., K. F. Xu, Q. Fan, G. Pacheco-Rodriguez, J. Moss et al., 2006   Association of brefeldin A-inhibited guanine nucleotide-exchange protein 2 (BIG2) with recycling endosomes during transferrin uptake. Proc. Natl. Acad. Sci. USA 103: 2635–2640. https://doi.org/10.1073/pnas.0510599103

Shieh, B. H., 2011   Molecular genetics of retinal degeneration: A *Drosophila* perspective. Fly (Austin) 5: 356–368. https://doi.org/10.4161/fly.5.4.17809

Shin, H. W., N. Morinaga, M. Noda, and K. Nakayama, 2004   BIG2, a guanine nucleotide exchange factor for ADP-ribosylation factors: its localization to recycling endosomes and implication in the endosome integrity. Mol. Biol. Cell 15: 5283–5294. https://doi.org/10.1091/mbc.e04-05-0388

Shinotsuka, C., Y. Yoshida, K. Kawamoto, H. Takatsu, and K. Nakayama, 2002   Overexpression of an ADP-ribosylation factor-guanine nucleotide ex- change factor, BIG2, uncouples brefeldin A-induced adaptor protein-1 coat dissociation and membrane tubulation. J. Biol. Chem. 277: 9468–9473. https://doi.org/10.1074/jbc.M112427200

Tepass, U., and K. P. Harris, 2007   Adherens junctions in *Drosophila* retinal morphogenesis. Trends Cell Biol. 17: 26–35. https://doi.org/10.1016/j.tcb.2006.11.006

Wang, J., Y. Morita, J. Mazelova, and D. Deretic, 2012   The Arf GAP ASAP1 provides a platform to regulate Arf4- and Rab11-Rab8-mediated ciliary receptor targeting. EMBO J. 31: 4057–4071. https://doi.org/10.1038/emboj.2012.253

Wang, S., K. L. Tan, M. A. Agosto, B. Xiong, S. Yamamoto *et al.*, 2014 The retromer complex is required for rhodopsin recycling and its loss leads to photoreceptor degeneration. PLoS Biol. 12: e1001847. https://doi.org/10.1371/journal.pbio.1001847

Wang, Y., H. Zhang, M. Shi, Y. C. Liou, L. Lu *et al.*, 2017 Sec71 functions as a GEF for the small GTPase Arf1 to govern dendrite pruning of *Drosophila* sensory neurons. Development 144: 1851–1862. https://doi.org/10.1242/dev.146175

Xiong, B., and H. J. Bellen, 2013 Rhodopsin homeostasis and retinal degeneration: lessons from the fly. Trends Neurosci. 36: 652–660. https://doi.org/10.1016/j.tins.2013.08.003

Yamaji, R., R. Adamik, K. Takeda, A. Togawa, G. Pacheco-Rodriguez *et al.*, 2000 Identification and localization of two brefeldin A-inhibited guanine nucleotide-exchange proteins for ADP- ribosylation factors in a macromolecular complex. Proc. Natl. Acad. Sci. USA 97: 2567–2572. https://doi.org/10.1073/pnas.97.6.2567

Zelhof, A., R. W. Hardy, A. Becker, and C. S. Zuker, 2006 Transforming the architecture of compound eyes. Nature 443: 696–699. https://doi.org/10.1038/nature05128

Zhao, X., T. K. Lasell, and P. Melançon, 2002 Localization of large ADP-ribosylation factor-guanine nucleotide exchange factors to different Golgi compartments: Evidence for distinct functions in protein traf c. Mol. Biol. Cell 13: 119–133. https://doi.org/10.1091/mbc.01-08-0420

Communicating editor: B. Andrews